Experimental analysis of damage creation and permanent indentation on highly oriented plates

Elias Abi Abdallah [a], Christophe Bouvet [b,*], Samuel Rivallant [a], Bernhard Broll [a], Jean-Jacques Barrau [b]

[a] Université de Toulouse/ISAE/DMSM, 10 av. E. Belin, 31055 Toulouse cedex, France
[b] Université de Toulouse/UPS/LGMT, 118 route de narbonne, bat 3PN, 31062 Toulouse cedex 04, France

A B S T R A C T

This paper presents an experimental investigation concerning low-velocity impact and quasi-static indentation tests on highly oriented laminates used in aeronautical and aerospace applications. The damage observed in such laminates is very particular. Post mortem analysis were carried out which helped to define an impact damage scenario. Microscopic observations led to explain the mechanism of permanent indentation formation which is a fundamental point of damage tolerance justification. Equivalence between static and dynamic is also discussed.

Keywords:
B. Impact behaviour
C. Damage tolerance
B. Matrix cracking

1. Introduction

The use of composite materials in aeronautical and aerospace applications has been increasing recently because of their stiffness to weight and strength to weight ratio. During composite structure's life, low-velocity impacts by foreign objects may occur during manufacturing, maintenance, operation, etc, which can largely affect their residual mechanical properties [1]. Even if there is no damage sign on the surface, however, internal defects may already have been created [2]. The minimum damage that can be detected by visual evaluation is the Barely Visible Impact Damage (BVID) [3]. In aeronautical standards, the threshold of detectability after few days of rest and humidity aging is 0.3 mm of dent depth. In this study, the BVID is taken as 0.6 mm after 48 h of relaxation but without humidity aging which can decrease more the depth of the indentation.

Therefore, in order to cope with safety standards, designing and dimensioning composite structure require taking into account damage tolerance [4,5]. Damage tolerance was introduced in 1978 in the civil aviation. This requirement is explicitly expressed by the standard JAR 25.571: "the damage tolerance evaluation of the structure is intended to ensure that should serious fatigue, corrosion, or accidental damage occur within the operational life of the airplane, the remaining structure can withstand reasonable loads without failure or excessive structural deformation until the damage is detected".

In the field of impact damages, the damage tolerance drives to dimension the structure depending on the impact detectability: if the damage is not detectable, practically when the impact indentation is less than BVID, the structure must support the extreme loads and if the damage is detectable, practically when the impact indentation is bigger than BVID, an other criterion must be considered [5]. The last case is not discussed in this paper.

The damage tolerance concept is fundamental because it leads to dimension the aeronautics structures, not only by comparing their strength to the applied external forces but also by taking into account their capacity to keep track of the impact. This capacity to mark during an impact must be considered during the structure design.

Consequently, the damage tolerance has been a subject of investigation for many years. Several authors [6–9] have been studying the response of composite structures to low-velocity impact. They have been trying to give an explanation and to simulate the different damage phenomena appearing during these tests. However, more research studies are still needed to be performed to have better understanding of the damage phenomena developed in these materials during impact but equally to better explain and simulate the indentation phenomenon which is fundamental in damage tolerance design. Paradoxically, in authors knowledge, this indentation phenomenon has not been subject of investigations in the literature and the attempted explanation proposed in this paper might be quite original.

In this paper, a study of the impact behaviour of highly oriented plates, used in special aeronautical and aerospace applications, was carried out. Impact and quasi-static tests were performed to monitor the damage creation and development during these experiments. A comparison between these two tests is also treated with the aim in replacing the dynamic analysis by static one because much more

* Corresponding author. Address: Université Paul Sabatier, Filière Génie Mécanique, Bât. 3PN, 118, route de Narbonne – 31062 Toulouse cedex 04, France. Tel.: +33 (0) 5 61 55 84 26; fax: +33 (0) 5 61 55 81 78.
E-mail address: bouvet@lgmt.ups-tlse.fr (C. Bouvet).

data can be obtained from these tests than from an impact one. This subject was investigated by many researchers [10–13]. These authors demonstrated a good behaviour resemblance for these two tests.

2. Experimental setup

2.1. Materials

RTM laminates were manufactured with 12 layers of carbon fibres of the type G30-500 GK HTA-76 produced by Toho Tenax and infused with epoxy resin RTM6 delivered by Hexcel Composite. Two nearly balanced woven fabric layers of 0.2 mm thickness were placed on the upper and lower surface of the plate at the longitudinal direction. Between these two layers, 10 quasi unidirectional (quasi UD) layers of 0.3 mm thickness were draped and aligned along the longitudinal direction (cf. Fig. 1). This quasi UD is a woven fabric with all carbon fibres placed in the warp direction and only holding threads, made of glass, placed in the weft direction .The materials properties of the two different layers were evaluated experimentally and are listed in Table 1.

El_t and El_c are the Young modulus in tension and compression through the fibres directions while Et_t and Et_c are the Young modulus in traction and compression in the transverse directions. σl_t and σl_c are the failure stresses in traction and compression through the fibres directions while σt_t and σt_c are the failure stresses in traction and compression in the transverse direction. τlt, Glt and υlt are the failure shear stress, the shear modulus and the Poisson's ratio in the l–t plane, respectively.

2.2. Low-velocity impact and quasi-static indentation tests

The tested plates were cut into specimen of $150 \times 100\ mm^2$ in dimensions and impacted with different energies. Low-velocity impact tests were conducted using a guided drop weight tester (cf. Fig. 2). The principle of free fall weight is to drop an instrumented mass (impactor) from a specific height on a specimen held by a support (cf. Fig. 3). The drop weight tester presented in Fig. 2 consists of a main block of 4 kg, a spherical indentor having a 12.7 mm diameter, a piezoelectric force sensor and an accelerometer to measure the impact load and acceleration during the test, respectively. An optical sensor is used in order to evaluate the initial velocity before the impact. All the results are collected by an analogical data acquisition system [14]. Then the force/displacement curve is plotted which gives an idea of impact plates behaviour (cf. Fig. 4). The impact energy is the area occupied by this curve.

Quasi-static tests were performed by an INSTRON testing machine at a displacement rate of 0.5 mm/min with the aim of comparing the behaviour of the indented and impacted plate. The same spherical indentor as the one utilized for impact tests was used. These tests were done at the same maximum displacement attained by the impactor during the dynamic experiments for comparing them. They were performed at different displacements to study and evaluate the creation and the development of the different damages.

Some of the impacted and indented plates were subjected to non destructive controls as X-rays to define the damaged zone obtained after the tests. Afterwards, destructive controls (microscopic observation) were done in order to identify a damage scenario which will be lately developed in the paper.

3. Experimental results

3.1. Force–displacement curve

In Fig. 4, force–displacement curves for plates tested statically and dynamically at two different loading are presented. It can clearly be seen, for the plate tested at the maximum energy, that the force–displacement curve can globally be divided into four big parts. The first part of the graph is linear which represents the rigidity of the non damaged specimen. At around 0.8 mm (A), the linearity is lost which can give an indication of damage initiation. At around 1.4 mm displacement (B), a brutal decrease of the force is observed, however, the force is still increasing until it reaches a maximum between 5 and 5.5 mm depending on the tests (C). Afterwards, this forces starts to decrease awaiting the test end (D). These observations will be detailed in the impact damage scenario paragraph. Moreover this scenario description is more specifically based on data (curves and micrographs) obtained during static tests, in order to benefit from greater clarity of static curves. Afterwards a comparison between static and dynamic cases is treated (cf. Section 3.4).

3.2. Damage scenario

As mentioned before, plates impacted at different impact energies and others statically tested at the same maximum displacement reached during the dynamic experiment were submitted to microscopic observations in order to explain the creation and propagation of the damage during these tests. By visual inspection, three different cracks can be monitored on the surface and the bottom of the specimen (cf. Figs. 5 and 6). These three crack types, named 1, 2 and 3 in the following of the text, are equally visible on the X-rays (cf. Fig. 12) performed on the impacted and indented plates. Later (48 h), the permanent indentation is measured for each tested plates which were later enrobed by an inclusion resin in order to prevent the relaxation of the damaged parts after cutting them. Then two different cuts were done (cf. Fig. 5) to observe

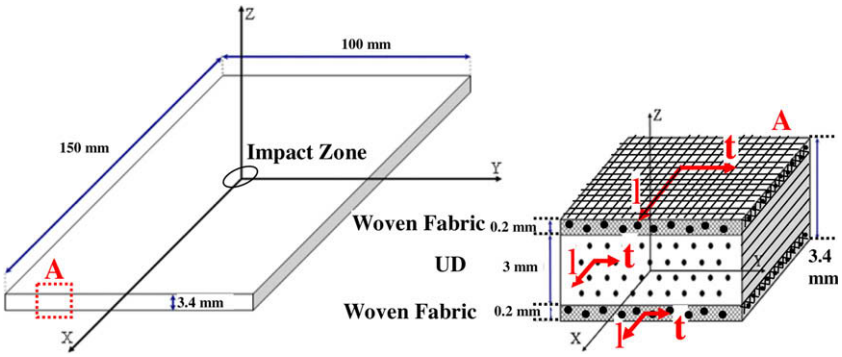

Fig. 1. Plates stacking sequence and dimensions.

Table 1
Materials properties.

	El_t (GPa)	Et_t (GPa)	El_c (GPa)	Et_c (GPa)	σl_t (MPa)	σt_t (MPa)	σl_c (MPa)	σt_c (MPa)	τlt (MPa)	Glt (GPa)	υlt
Woven fabric	60	55	47	49	792	639	571	480	64	3.15	0.07
Quasi UD	108	8	87	8	1407	52	886	228	94	2.94	0.3

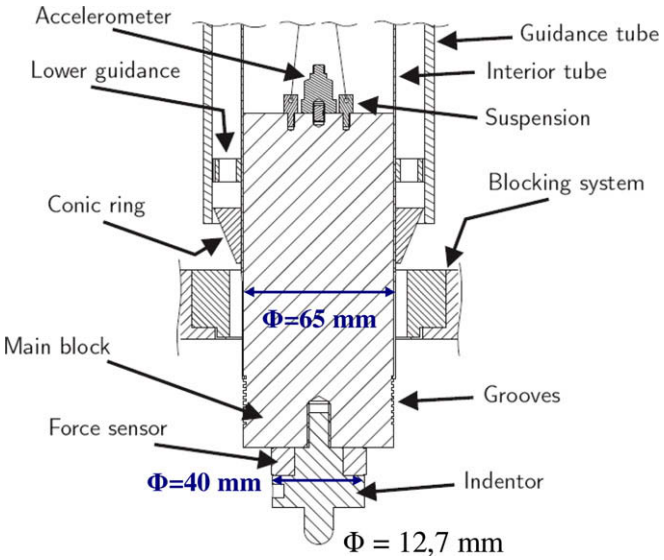

Fig. 2. The drop weight tester.

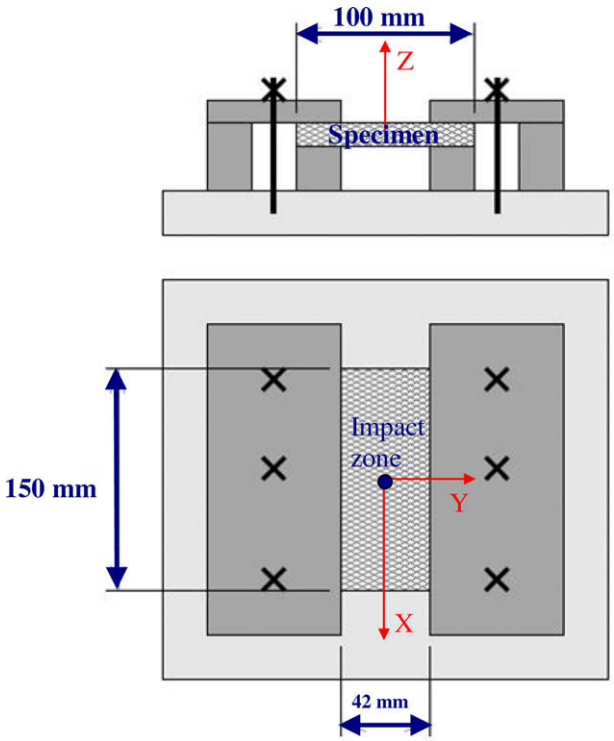

Fig. 3. The support system.

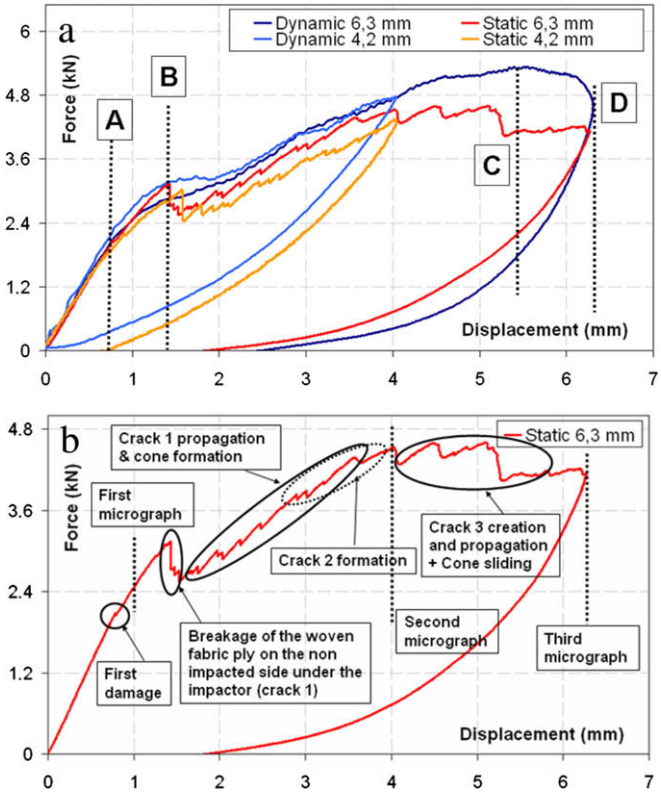

Fig. 4. Force/displacement curves of dynamic and static tests.

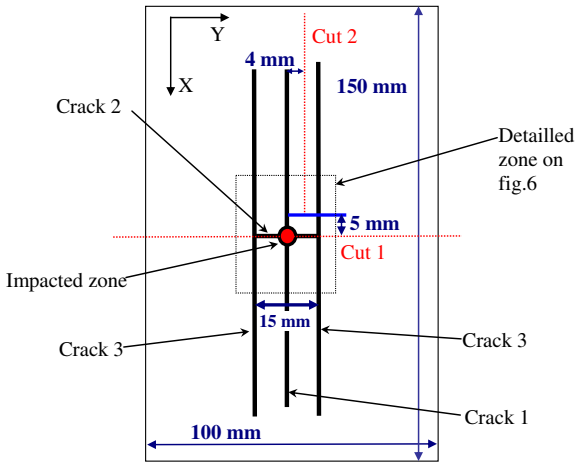

Fig. 5. The different cuts realized for microscopic observations.

microscopically the shape of these cracks. Figs. 5 and 6 show the different damages developed in the tested plates. The chronological appearance of these cracks is detailed later.

3.2.1. From 0 to 1 mm of maximum displacement

From 0 to 0.8 mm of maximum displacement, material graph is linear which represents the rigidity of the non damaged specimen (cf. Fig. 4). At around 0.8 mm (A), the linearity is lost which means damage initiation. The damages at 1 mm of displacement consist in

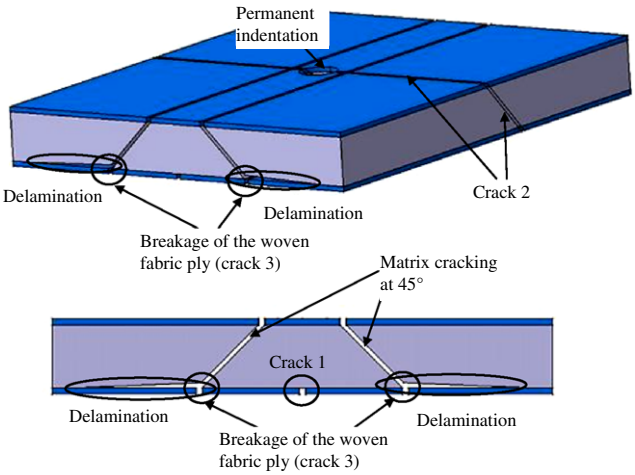

Fig. 6. The different damages developed during the impact and quasi-static indentation tests on the tested plates.

matrix cracking developing in a conical shape from the non-impacted side and propagating toward the impacted side of the specimen (cf. Fig. 7). This micrograph (cf. Fig. 7), obtained with the cut one parallel to the *Y* axis (cf. Fig. 5), shows equally the first ply at the impacted side is torn which is the local crushing. Moreover, a delamination also appears between the last and before last ply (cf. Fig. 7).

3.2.2. From 1 to 4 mm of maximum displacement

At 1.4 mm of displacement a brutal decrease of the force appears (cf. Fig. 4). It is probably due to the breakage of the woven fabric ply under the impactor at the non-impacted side (cf. Fig. 8). The evolution of this crack, named 1 in the following of the text (cf. Fig. 6), is equally plotted in Fig. 9 and is visible on X-rays (cf. Fig. 12). The propagation of this crack 1 is probably responsible of the little decreases of the force between 1.4 and 4 mm (cf. Fig. 4). Between these two displacements, .the conical damage observed at 1 mm continues to develop through the thickness until reaches the surface of the specimen at maximum displacement of around 4 mm (cf. Fig. 8). Furthermore, other cracks start to appear from the surface of the plates and propagate to the bottom part which can be explained by the increasing contact between the spherical indentor and the specimen forming a bigger damage cone. This conical damage expands more and more through the length of the specimens (*X* direction) with the increasing of the displacement. Moreover, the opening of these cracks at 45° is also growing in *Z* direction with the increasing of the displacement because of the moving of the conical part limited by these cracks in this direction. In addition to the conical damage, the delamination presents between the last and before last ply, is developing throughout the width of the plates. A permanent indentation begins equally to appear (cf. Fig. 13) due to the development of these damages. Moreover a new crack, named 2 (cf. Fig. 6), oriented at 45° through the thickness of the plate appears just before 4 mm (cf. Fig. 9) and propagates in the *Y* direction. It starts at the end of the contact between the indentor and the plate and is perpendicular to the first crack (cf. Fig. 6). It is equally visible on X-rays (cf. Fig. 12) and can be observed thanks to a micrographic cut parallel to the *X* axis (cf. Fig. 5) and near the impact point (cf. Fig. 11).

3.2.3. From 4 to 6.3 mm of maximum displacement

Just after 4 mm of displacement a brutal decrease of the force appears (cf. Fig. 4). It is probably due to the breakage of the first ply of the non-impacted side, which is a woven fabric, at the end of the conical shape damage (cf. Fig. 10). The evolution of this crack, named 3 in the following of the text (cf. Fig. 6), is equally plotted in Fig. 9 and is visible on X-rays (cf. Fig. 12). Its strong propagation between 4 and 6.3 mm (cf. Fig. 9), is probably responsible of the successive decreases of the force (cf. Fig. 4). It can be noted that its precise evolution is not known but only its lengths at 4 and 6.3 mm. This crack 3 gets the central part of the plate completely detached in a conical shape (cf. Fig. 10) and seems to discharge the crack 2. In effect, this crack 2 stops to evaluate just after the crack 3 appearing (cf. Fig. 9). Moreover, this crack 3 seems to be responsible of the strong evolution of the permanent indentation after 4 mm (cf. Fig. 13) due to the sliding of the central cone.

3.3. Permanent indentation formation

As mentioned before, the damage presents three different cracks 1, 2 and 3. Micrograph 3 (cf. Fig. 10) shows the damage developed at the maximum displacement at which these plates were tested. This micrograph shows the breakage of the woven fabric ply at the non-impacted side at the end of the crack at 45°. This ply has a big role of holding the part under the cone from getting completely detached. This hypothesis is confirmed by the strong evolution of crack 3 length near 4 mm displacement (cf. Fig. 9) and by the evolution of the permanent indentation at this same displacement (cf. Fig. 13). In effect this permanent indentation, measured after 48 h of relaxation shows a strong increase at around 4 mm displacement when the crack 3 is formed. After the formation of crack 3, the part under the cone continues to slide

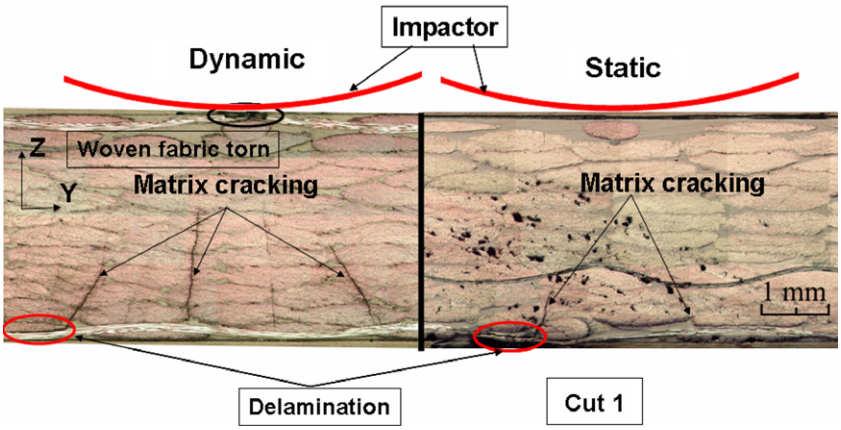

Fig. 7. Microscopic photos of a test at 1 mm of maximum displacement. Dynamic and static tests.

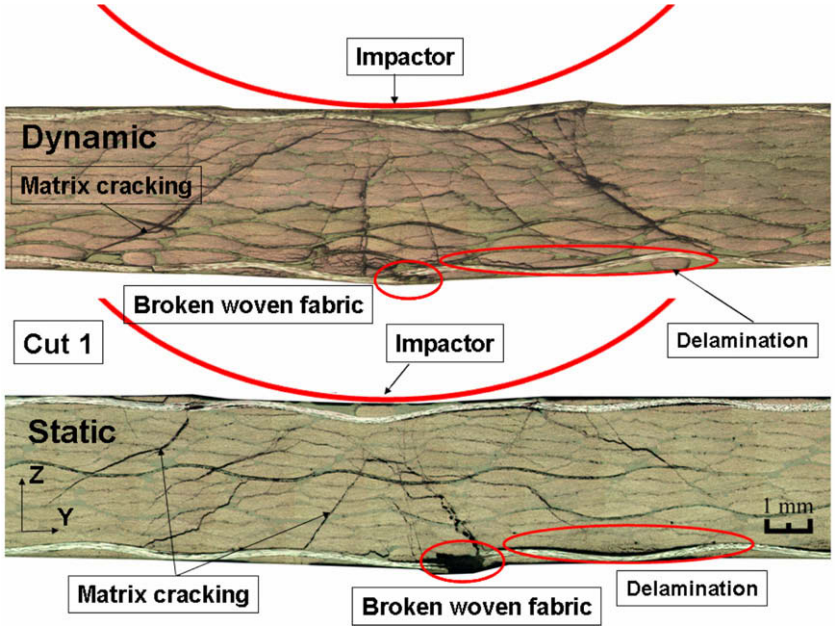

Fig. 8. Microscopic photos of a test at 4 mm of maximum displacement. Dynamic and static tests.

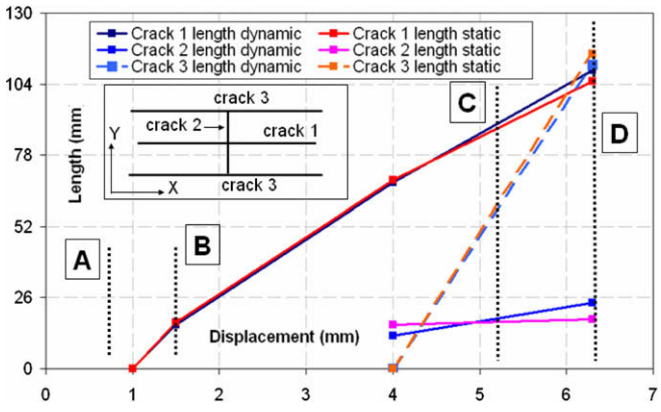

Fig. 9. Evolution of cracks 1, 2 and 3 lengths in dynamic and static tests.

down (cf. Fig. 10) which increase the opening of the cracks at 45° letting the debris get in. In Fig. 14, it can be noticed that these debris caused from fibre and resin rupture get stuck in these cracks and creates a sort of blocking system that prevents this detached part of the specimen which is under the cone from getting back to zero level after the impact which creates a mark at the surface of the specimen. More the crack is opened, more debris can get in which can lead to an increasing of the indentation. This mechanism is fundamental in creating the permanent indentation.

In order to verify this mechanism, microscopic observations were performed on other type of plates. The material used for the fabrication of these plates is T700/M21. These laminates of $150 \times 100\,mm^2$ are fabricated with 16 unidirectional plies with this stacking sequence $[0°_2,45°_2,90°_2,-45°_2]_S$. They were clamped by a $125 \times 75\,mm^2$ window and impacted at 5.1 mm of maximum displacement. As for the highly oriented plates, these plates were enrobed after relaxation by an inclusion resin in order to be cut

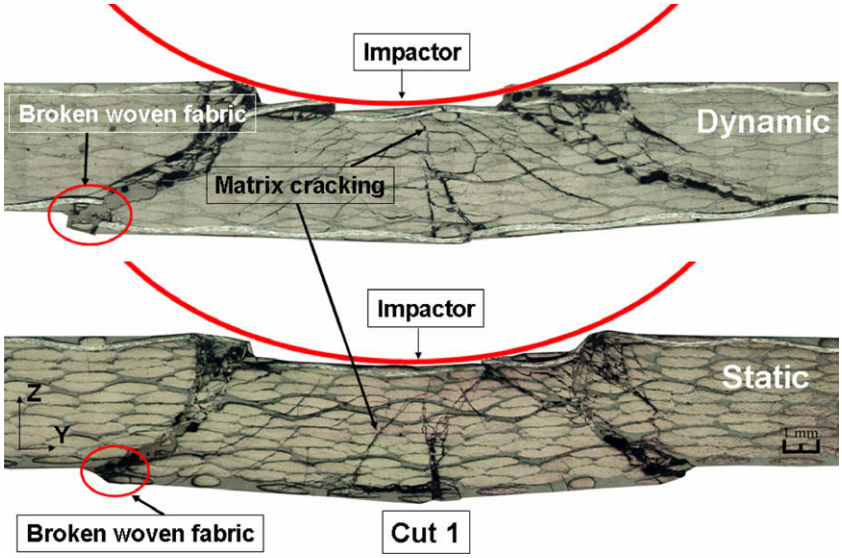

Fig. 10. Microscopic photos of a test at 6.3 mm of maximum displacement. Dynamic and static tests.

Fig. 11. Crack 2 development at 6.3 mm of maximum displacement.

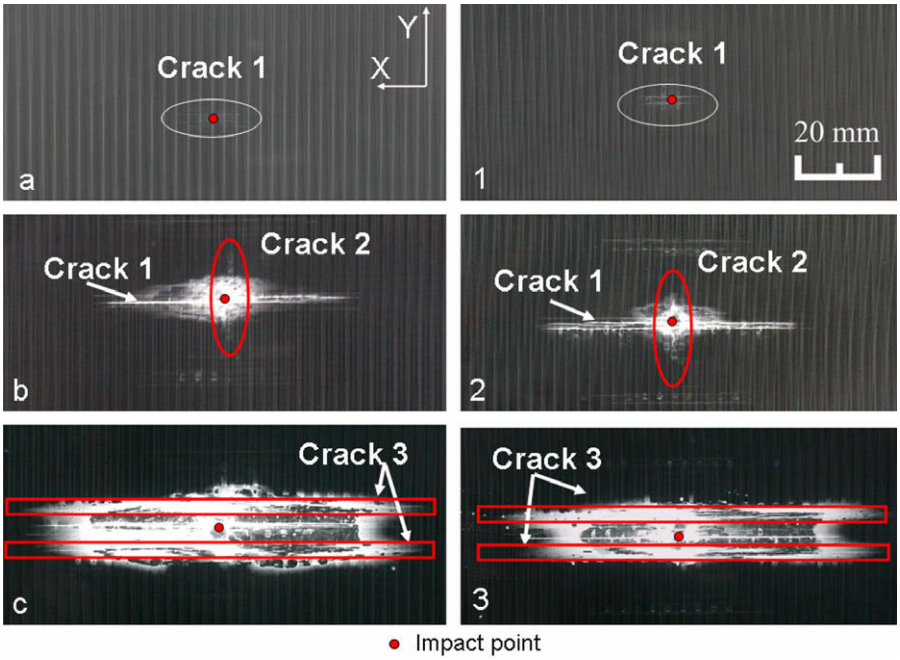

Fig. 12. The X-rays of the tested plates: (a, 1) plates impacted and indented at 1.5 mm displacement, respectively. (b, 2) Plates impacted and indented at 4 mm displacement, respectively. (c, 3) Plates impacted and indented at 6.3 mm displacement, respectively.

and submitted to microscopic observation. Fig. 15 presents a microscopic photo of an impacted plate and also shows the presence of debris in the different cracks. These observations can confirm that the non return of the damaged part is due to the presence of the debris that get infiltrated in the different cracks and create a blocking system.

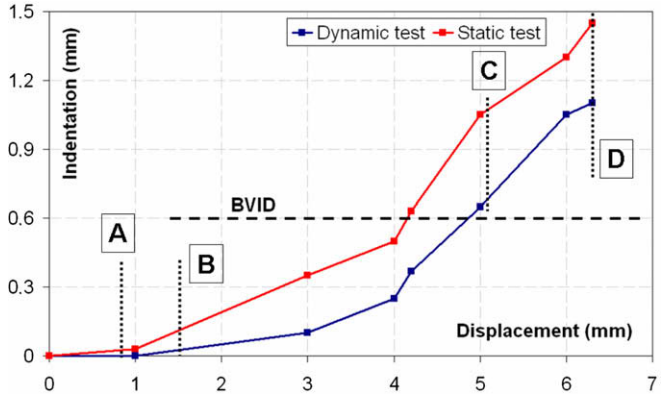

Fig. 13. The difference of indentation between the dynamic and static tests after 48 h of relaxation.

3.4. Static/dynamic comparison

Low-velocity impact and quasi-static indentation tests were carried out to compare the behaviour of the composite laminate to different loadings.

Fig. 4 represents a comparison between static and dynamic force–displacement curves. It can be remarked that the curves have the similar shape globally for both tests.

It can be noticed that the force attained during the impact test is always greater than the one obtained during the static one (cf. Fig. 4). In authors knowledge, there is no explication of that phenomenon in the literature. On the contrary, other authors [15–17] have even obtained opposite results. In Fig. 16, the total energy applied during the different tests versus the displacement is plotted. This energy is divided in two parts, the elastic and absorbed one. The total energy reached during the low-velocity impact test is always greater than the static one for the same impactor displacement (cf. Fig. 16), like it was for the resulted

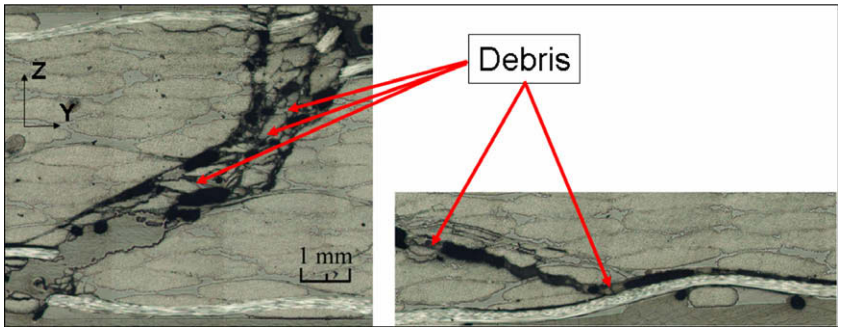

Fig. 14. Photos of the debris blocking the return to zero in a specimen tested at 6.3 mm of maximum displacement (details of Fig. 10).

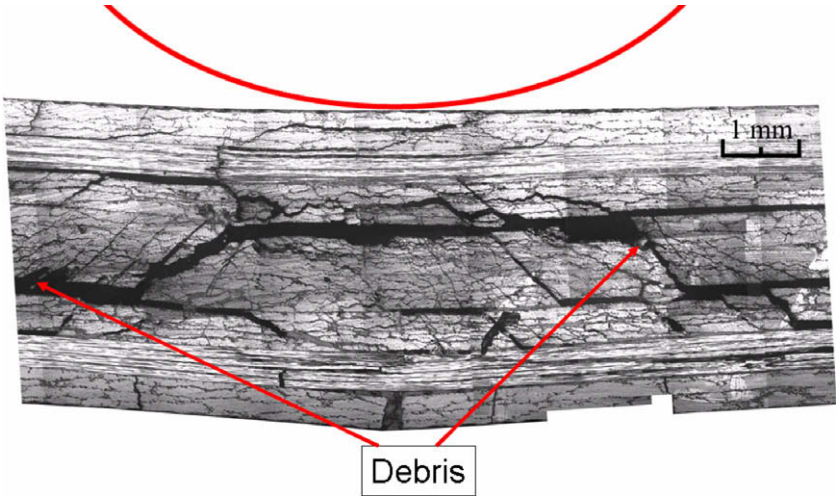

Fig. 15. The debris presented in the different cracks caused by an impact test on a plate with different fibers orientation.

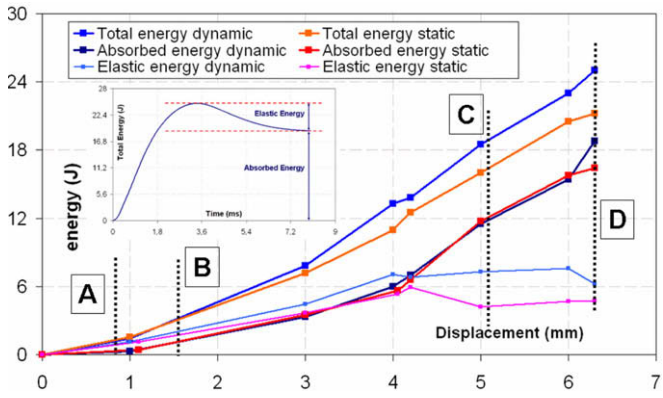

Fig. 16. Total, absorbed and elastic energies during the static and dynamic tests.

force. Nevertheless, the absorbed one is equivalent for static and dynamic cases which means there is equivalence in term of damage in these two tests at the same imposed displacement. This result is equally visible on the X-rays observations (cf. Fig. 12), microscopic photos (cf. Figs. 7, 8 and 10) and cracks length evolutions (cf. Fig. 9).

However, the permanent indentation caused by these tests is quite different (cf. Fig. 13). In Fig. 13, the permanent indentation after relaxation is plotted in function of the maximum displacement of the indentor. It can be noticed that the indentation caused by the static tests is greater than the one cause by the dynamic tests even if the damages formed is quite similar, which was not mentioned before in the literature, in authors knowledge. This phenomenon can be explained by the fact that, during the static test, the debris have much more time to displace and get installed in the different cracks, however, it is not the case during the impact tests.

4. Conclusion

Specific damages in highly oriented plates along the longitudinal direction formed with two different layers, woven fabric and quasi UD, have been observed. A damage scenario for these plates was proposed. It consists of the development of matrix cracks, starting from the non-impacted side, which develop in a conical form through the thickness of the specimen. A first crack consisting of a break in the woven fabric layer in the non-impacted side of the plate creates and propagates in the longitudinal direction. The delamination is equally present between the last and before last ply. A second crack is also developed through the thickness at 45° perpendicular to the first one and propagates in the transverse direction. Two third cracks which are the breakage of the woven fabric ply presented at the surface of the non-impacted side of the specimen at the end of the 45° crack create and propagate in the longitudinal direction.

Moreover, a comparison between static and dynamic tests was treated in this paper. The maximum force attained during the impact tests is greater than the one during the quasi-static tests. Nevertheless, the absorbed energy and damage morphologies are equivalent for both tests.

However, the indentation left from these tests is quite different and it is important to mention that the static tests mark more than the dynamic ones. This phenomenon can be explained by the fact that the static tests last longer than the dynamic one and the debris formed from the different damages developed through the test have more time to sneak in the different cracks and create a sort of blocking system to prevent the different parts from getting back to their initial position. Therefore, the mechanism of blocking plays an essential role of forming the BVID which is fundamental in damage tolerance.

The better understanding of the permanent indentation mechanism should allow improving the design of composite structures to damage tolerance. This understanding is fundamental to better use composite materials in aeronautical and aerospace structures.

References

[1] Abrate S. Impact of composite structures. Cambridge (UK): Cambridge University Press; 1998.

[2] Zhang ZY, Richardson MOW. Low velocity impact induced damage evaluation and its effect on the residual flexural properties of pultruded GRP composite. Compos Struct 2007;81:195–201.

[3] Moody RC, Harris JS, Vizzini AJ. Width effects on the compression strength of composite sandwich test specimens after barely visible impact damage. AIAA-99-1436; 1999. p. 1984–92.

[4] Coutellier D, Walrick JC, Geoffroy P. Presentation of a methodology for delamination detection within laminated structures. Compos Sci Technol 2006;66:837–45.

[5] Alderliesten RC. Damage tolerance of bonded aircraft structures. Int J Fatigue 2008;1:1–10. doi:10.1016/j.ijfatigue.2008.05.00.

[6] Li CF, Hu N, Cheng JG, Fukumaga H, Sekine H. Low-velocity impact-induced damage of continuous fiber-reinforced composite laminates. Part II. Verification and numerical investigation. Compos: Part A 2002;33:1063–72.

[7] Ballère L, Viot P, Lataillade J-L, Guillaumat L, Cloutet S. Damage tolerance of impacted curved panels. Int J Impact Eng 2008. doi:10.1016/j.ijimpend.2008.03.004.

[8] Mitrevski T, Marshall IH, Thomson R. The influence of impactor shape on damage to composite laminates. Compos Struct 2006;76:116–22.

[9] Davies GAO, Zhang X. Impact damage prediction in carbon composite structures. Int J Impact Eng 1995;16(1):149–70.

[10] Known YS, Sankar BV. Indentation flexure and low velocity impact damage in graphite epoxy laminates. J Compos Technol Res 1993;15(2):101–13.

[11] Kaczmarek H, Maison S. Comparative ultrasonic analysis of damage in CFRP under static indentation and low velocity impact. Compos Sci Technol 1994;51:11–26.

[12] Sjoblom PO, Hartness TJ, Cordell TM. On low velocity impact testing of composite materials. J Compos Mater 1988;22:30–52.

[13] Nettles AT, Douglas MJ. A comparison of quasi-static indentation to low velocity impact. NASA/TP-2000-210481; 2000.

[14] Petit S, Bouvet C, Bergerot A, Barrau JJ. Impact and compression after impact experimental study of a composite laminate with cork thermal shield. Compos Sci Technol 2007;67:3286–99.

[15] Suh SS, Han NL, Yang JM, Hahn HT. Compression behavior of stitched stiffened panel with clearly visible stiffener impact damage. Compos Struct 2003;62:213–21.

[16] Belingardi G, Vadori R. Influence of the laminate thickness in low velocity impact behavior of composite material plate. Compos Struct 2003;62:27–38.

[17] Nettles AT, Hodge AJ. The impact response of carbon/epoxy laminates. NASA/TM-97-206317; 1997.